Phase Effects on the Polymerization of a Styrloxy Cholesteric Liquid Crystalline Monomer

S. E. Williamson, D. Kang, and C. E. Hoyle*

Department of Polymer Science, The University of Southern Mississippi, Box 10076, Hattiesburg, Mississippi 39406-0076

Received June 13, 1995; Revised Manuscript Received June 17, 1996[⊗]

ABSTRACT: A styryloxy liquid crystalline monomer was synthesized and photopolymerized via free radical and cationic initiators with continuous and pulsed light sources. A phase description of monomer/polymer mixtures was used to help assist in the interpretation of the polymerization data. The monomer (a cholesteryl ester) exhibits isotropic, cholesteric nematic, and crystalline phases. For conversions of up to about 20% polymer, the polymerization media appear to exhibit the same cholesteric phase as the monomer, allowing polymerization rates to be measured in a purely cholesteric nematic phase. Free-radical polymerization exotherms show rate accelerations at conversions corresponding to compositions where changes are observed in the medium opacity. No accelerations are observed for cationic polymerization: Differences are attributed to the types of termination processes in free-radical and cationic polymerization. While polymerization rate changes differ for the free-radical and cationic polymerizations, real-time laser light scattering indicates that polymerization induced phase changes occur at the same degree of conversion in both cases. Rates for free-radical polymerization were also measured as a function of temperature. Arrhenius plots indicate that the polymerization activation energy at low conversions is the same for polymerization in the cholesteric nematic and isotropic phases.

Introduction

Due to a number of potential applications which utilize films with liquid crystalline-type ordering, a great deal of interest has been exhibited in the polymerization of thermotropic liquid crystalline monomers and of isotropic monomers in inert liquid crystalline solvent media.[1−21] Recently, for difunctional liquid crystalline monomers which produce cross-linked networks, Broer et al. (refs 6−9 and references therein) have shown that liquid crystalline order has little, if any, effect on the polymerization rate. For a monofunctional methacrylate monomer with a decoupled side chain mesogenic cholesterol group (CMA-10), Hoyle and co-workers[10−14] have shown that the rate of polymerization at low conversions in a homogeneous smectic A phase is markedly higher than in the isotropic phase. The restricted mobility of the smectic A medium resulted in a polymerization rate increase due to a significant decrease in the measured termination rate constant relative to the isotropic phase: The propagation rate constant was found to be virtually independent of the phase ordering. A survey of the pertinent literature[5,15−18] for monofunctional liquid crystalline monomers indicates that the exact effect of nematic ordering on polymerization rates is not obvious and must be assessed on a case by case basis. Also, phase changes during polymerization may make interpretation of kinetic data difficult. For example, at temperatures where the pure monomer CMA-10 was initially a cholesteric nematic, a medium phase change occurred at low conversions upon polymerization. This precluded measurement of the polymerization rate in the pure cholesteric nematic medium. Interestingly, however, a rate acceleration, attributed to a decrease in the termination rate relative to the propagation rate, accompanied the medium phase change.[14] Broer et al. also reported that the free-radical polymerization of a monofunctional liquid crystalline acrylate with a biphenyl side group from the monomer nematic phase resulted in polymer phase separation in the early stages of polymerization.[5] They suggested that the smectic order of the phase separated polymer resulted in a decrease in termination rate and a faster polymerization rate.[5] Hence, as in the case of the CMA-10 monomer, it was difficult to observe polymerization in a pure nematic phase over a significant conversion range.

In contrast to the results for free-radical polymerization in liquid crystalline media, very little has been reported[11,19] about the effects of liquid crystalline ordering on cationic polymerization, even though the comparison between cationic and free-radical polymerization has interesting mechanistic implications due to fundamental differences in the termination mechanisms. In radical polymerization, termination is bimolecular with respect to the reactive polymer chain concentration, and thus highly dependent upon the diffusion rate of the polymer chain. For cationic polymerization, however, termination is unimolecular with respect to the reactive polymer chain concentration, and therefore much less affected by medium viscosity.

Two questions arise from previous work on polymerization in liquid crystalline mesophases. First, does polymerization in a pure cholesteric nematic phase proceed more, or less, rapidly that in an isotropic phase? After all, nematic phases are intermediate in order between smectic and isotropic phases. Since nematic phases have only orientational order and not positional/orientational ordering like smectic phases, the free-radical polymerization rate, which is dictated in large part by diffusion controlled bimolecular coupling, may well not be affected to any great extent by cholesteric nematic ordering. Second, do phase changes which occur during polymerization from initially isotropic or cholesteric nematic phases lead to rate acceleration for chain-growth cationic polymerizations as well as free-radical polymerization? Since chain-growth cationic polymerization does not proceed by a bimolecular termination process involving two growing polymer chains, it may be anticipated that it will not be influenced by the same medium order changes which affect free-radical polymerization kinetics.

[⊗] Abstract published in *Advance ACS Abstracts,* August 1, 1996.

S0024-9297(95)00826-6 CCC: $12.00

The CSE-10 monomer, identical in structure to CMA-10 except for a polymerizable styryloxy functionality, provides a means to answer these two questions. CSE-10 and its mixtures of up to 20% polymer (derived from polymerization of CSE-10) exhibit a broad cholesteric phase, allowing the opportunity to investigate polymerization kinetics in the homogeneous cholesteric nematic phase without phase separation over a wide temperature and composition range (0−20% conversion). Determination of the effect of the cholesteric nematic mesophase on the rate of polymerization can thus be made at low conversions without complicating phase changes. Furthermore, CSE-10 may polymerize by either a free-radical or a cationic process, thus providing the opportunity for a direct rate comparison between free-radical and cationic polymerization rate changes resulting from medium phase changes occurring during polymerization.

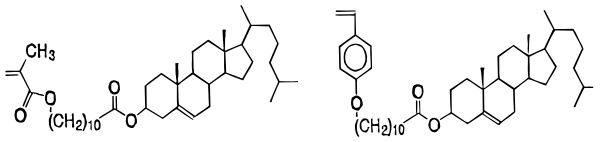

CMA-10 CSE-10

Experimental Section

Reagents and Solvents. The radical photoinitiator, 2,2-dimethoxy-2-phenylacetophenone (DMPA or Irgacure 651, Ciba-Geigy) was recrystallized from *n*-hexane prior to use. The cationic photoinitiator, a 50% solution of a mixture of two triaryl aryl sulfonium salts [4,4′-bis(diphenylsulfonio)diphenyl sulfide hexafluoroantimonate and 4-(phenylthio)-4′-phenyldiphenylsulfonium hexafluoroantimonate] in propylene carbonate (UVI-6974, Union Carbide), and the radical inhibitor, hydroquinone (Aldrich), were used as received. *p*-Acetoxystyrene (Hoechest Celanese) and 11-bromoundecanoyl chloride (Alfa) were also used as received. Cholesterol (Aldrich) was recrystallized from ethyl acetate.

Synthesis and Characterization of 11-(Styryloxy)-undecanoate (CSE-10 Monomer). Cholesteryl 11-bromoundecanoate was synthesized from 11-bromoundecanoyl chloride and cholesterol according to the method of Shannon.[20,21] *p*-Hydroxystyrene was prepared by the saponification of *p*-acetoxystyrene as described by Corson et al.[22]

An excess of *p*-vinylphenol/*p*-hydroxystyrene (0.93 g, 0.008 mol), cholesteryl 11-bromoundecanoate (4.00 g, 0.006 mol), and anhydrous potassium carbonate (1.28 g, 0.01 mol) were mixed in 10 mL of dimethylforamide under nitrogen at room temperature. The mixture was refluxed at 100 °C for 3 h 15 min, cooled for 30 min, and then poured into deionized water, filtered, and washed until the pH of the wash water was neutral. After drying overnight in a vacuum oven, 3.89 g of the tan solid was recovered, which was dissolved in methylene chloride and dried with anhydrous magnesium sulfate (Aldrich). Pure product was obtained by repeated recrystallization from methylene chloride/methanol, followed by column chromatography (methylene chloride/silica gel). The pure white monomer is colorless in solution except for a bluish lyotropic phase formed in concentrated solutions in methylene chloride or chloroform. The product was characterized and structure verified by proton and carbon NMR, IR spectroscopy, differential scanning calorimetry (DSC), and light microscopy.

^{1}H-NMR ($CDCl_3$, TMS, δ, ppm): 6.9, 7.3 (2d, 4H, CH_2=CHAr*H*); 6.7 (d of d, 1H, CH_2=C*H*Ar); 5.1, 5.7 (2d, 2H, CH_2=CHAr); 5.39 (s, 1H, R_2C=C*H*R); 4.6 (b, 1H, R_2C*H*OC=O-); 3.9 (t, 2H, RCH_2OAr); _2.3 (6 H, C=CHCH_2R + ROC=OCH_2R); 2.1−0.65 (m, many H).

^{13}C-NMR ($CDCl_3$, TMS, δ, ppm): 173.3 (1C, R*C*=O-O-R); 158.9 (1C, *C*OCH_2-); 136.3 (1C, =*C*HAr); 130.2 (1C, =CH*C*Ar); 127.3 (2C, =CHArCHAr*C*-); 122.6 (1C, R_2C=*C*HR), 139.7 (1C, R_2*C*=CHR); 114.5 (2C, -CH_2OArCHAr*C*H-); 111.3 (1C, H_2*C*=CHAr); 73.7 (1C, R_2*C*HOC=OR); 68.0 (ArOCH_2R); 56.6, 56.1, 50.0 (3C, R_3CH); 50 < many peaks < 19.3 (1C, R_3C*C*H_3); 18.7 (1C, R_2CH*C*H_3); 11.8 (1C, R_3C*C*H_3). FTIR (KBr pellet): no peak at 3500−3000 cm^{-1} (Ar−OH); strong peaks at 2933, 2856, and 1733 cm^{-1} (C=O); moderate peaks at 1506, 1467, 1250, 1183, and 839 cm^{-1}.

Solution Polymerization. The PCSE-10 polymer for use in establishing monomer/polymer phase relationships was made by dissolving 0.25 g of CSE-10 monomer in 0.5 mL of benzene. AlBN was used as a thermal initiator, and the polymer was purified by repeated precipitation in methanol.

Phase Transitions. Thermal transitions of the monomer, polymer, and monomer/polymer mixtures were measured on a Perkin Elmer DSC 7 thermal analyzer (DSC) from the peak transitions at a heating and cooling rate of 10 °C/min, and were confirmed by polarized optical microscopy. For the monomer, repeated heating and cooling cycles reveal the same transitions when 100−300 ppm radical inhibitor (hydroquinone) was added to the monomer to prevent thermal polymerization. Phase transitions of samples prepared for photopolymerization were measured on the Perkin Elmer DSC-2B used to record polymerization exotherms and were consistent with those recorded for the pure monomer on the DSC 7. The actual phase in which photopolymerization occurred was determined on the DSC-2B upon cooling. Optical transitions of the monomers, polymers, and monomer/polymer mixtures were determined using either a Leitz Orthoplan polarizing light microscope or a Nikon Optiphot-Pol polarizing light microscope with a Mettler FP 52 hot stage.

Determination of Monomer/Polymer Phase Behavior. Phase behavior of the monomer/polymer system was determined by mixing known amounts of CSE-10 monomer with 4−75% PCSE-10 polymer produced by polymerization in solution [200−500 ppm radical inhibitor (hydroquinone) was added to prevent thermal polymerization of the monomer], and then measuring the transitions by optical microscopy and DSC as for the monomer. Thermal transitions (obtained on heating and on cooling from the melt) were first measured on the Perkin-Elmer DSC 7. For compositions of 20% polymer and below, where no melt phase separation was observed, thermal transitions were identical to those observed via optical microscopy. However, since the thermal transitions are very small, especially when more than one phase is present, light microscopy was used to determine the point at which the first change was observed in the mixtures (i.e., the first appearance of a polymer-rich liquid crystalline domain in the isotropic melt on cooling). Thermal transitions were observed for compositions above 20% polymer at the temperatures where a uniform liquid crystalline medium was observed via optical microscopy. Therefore, the phase texture identification and the presence of phase separation were determined by optical microscopic examination.

Polymerization Sample Preparation. The sample films (2−3 mg) were cast by injecting a concentrated (50%) methylene chloride or chloroform solution of the monomer, initiator, and inhibitor (cationic only) into indented degreased aluminum DSC pans (PL Laboratories x1021). The DSC pans were indented using a Perkin-Elmer crimper with a die modified to form a cup 0.64 mm deep and 4.0 mm in diameter, as described by Tryson and Schultz.[23,24] Free-radical polymerization was initiated with 1% (weight) DMPA initiator. Cationic polymerization was initiated with 2% (weight) triaryl sulfonium salt solution with 300 ppm (weight) hydroquinone added to prevent concurrent radical polymerization, as observed by Crivello.[25]

Treatment of Monomer Samples Prior to Photopolymerization. Prior to polymerization, all samples were purged with nitrogen in the isotropic phase (93 °C) for 3 min to remove oxygen, and then heated or cooled to the polymerization temperature, which was maintained for a brief time before polymerization (for example: about 2 min for samples polymerized at 69 °C, for a combined purge time of 5 min). Very little thermal polymer was observed (GPC) in samples heated to polymerization temperatures but not exposed to the lamp under these conditions. For consistency, the films for cationic polymerization were subjected to the same purge at the monomer isotropic temperature.

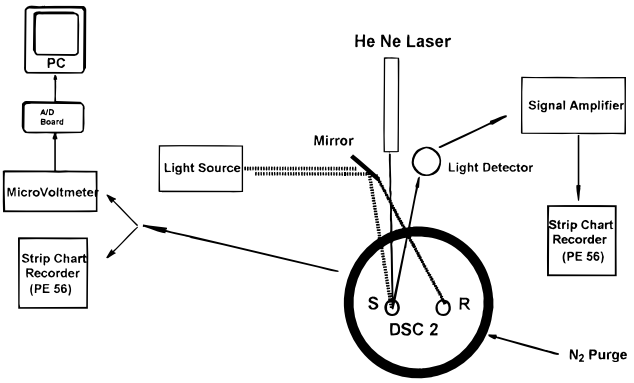

Figure 1. Equipment for photopolymerization in DSC with simultaneous HeNe laser transmitted light intensity measurements.

Polymerization Light Sources. The basic polymerization light source was a 450 W medium pressure mercury lamp (Canrad Hanovia). The intensity was controlled by various neutral density filters. A typical intensity of the Pyrex filtered lamp output was 14 mW/cm^2, while the intensity of the 366-nm filtered output was about 0.5 mW/cm^2 when no neutral density filters were used. The intensities of the light used to initiate photopolymerization are indicated in the figure captions. The pulsed light source used was a Questek Series 2000 Model 2460 pulsed excimer laser operating at the 351-nm line (XeF fill) at 17.9 mW/cm^2 and 5 Hz (17.9 mJ/cm^2, or 3.6 mJ/cm^2 per pulse). For photopolymerization on the microscope hot stage, the light source was the 365-nm band of a Spectroline Model ENF-240C lamp with a measured intensity of approximately 0.5 mW/cm^2 at 4.5 in. distance.

DSC Exotherm Unit. The polymerization kinetics were followed on a Perkin Elmer DSC-2B, modified as described in refs 12 and 13, with a quartz window to allow UV light penetration to the sample and reference pans. An enthalpy of polymerization for the styryloxy monomer of 70 kJ/mol[26,27] was used.

Real-Time Measurement of Transmitted Light Intensity Signal during Polymerization. To monitor, in real time (as polymerization progresses), the change in opacity (transparency) of the samples, the photo-DSC was configured as shown in Figure 1. The polymerization light source (a medium pressure mercury lamp) was reflected from the face of a mirror to the DSC sample holder. The intensity of light impinging on the sample and reference cells was balanced. A helium neon laser (633 nm) was positioned above the DSC so that the coherent beam from the laser impinged upon the sample in the DSC cell at a very low angle (less than 10°). The laser beam caused a small amount of local heating so that a slight displacement in the sample versus the reference signal from the DSC was recorded. The relatively diffuse laser light reflected off the bottom of the aluminum sample pan was focused by a lens onto a photodiode. The photodiode signal, amplified and recorded on a strip chart recorder, was then scanned and digitized for computer analysis.

Gel Permeation Chromatography. Polymer molecular weight distributions (relative to polystyrene standards) were determined on a gel permeation chromatography system (GPC) consisting of a Waters 6000A solvent delivery system, a Model 7010 Rheodyne injector, a Waters 410 differential refractometer, and four columns: a Shodex 10^6, and 100, 500, and 10^4 Å Waters Ultrastyragel columns. The nominal flow rate of the tetrahydrofuran mobile phase was 1 mL/min. The GPC system was calibrated with narrow molecular weight polystyrene (PS) standards from Polymer Laboratories and Polysciences. Elution volumes follow for several polystyrene molecular weight standards used for calibration: MW = 9000, V_e = 2086 mL; MW = 45 766, V_e = 1985 mL; MW = 90 000, V_e = 1828 mL; MW = 190 000, V_e = 1733 mL; and MW = 336 000, V_e = 1669 mL.

Results and Discussion

Since polymerization of liquid crystalline monomers may be dependent on both the medium phase and the extent of the monomer/polymer miscibility, we will first present a brief discussion of the monomer, polymer, and monomer/polymer phase behavior of CSE-10. The effect of the medium phase (isotropic versus cholesteric nematic) will then be presented for both cationic and free-radical polymerization. Rate changes will be correlated with corresponding changes in the medium as determined by simultaneous exotherm and HeNe laser light transmission measurements.

A. Phase Characterization of CSE-10 Monomer, PCSE-10 Polymer, and Monomer/Polymer Mixtures. Thermal and optical transitions of the pure CSE-10 monomer are as follows: On the first heating cycle, monomer cast from a methylene chloride solution melts at 68−69 °C to the cholesteric nematic phase [ΔH = 50 J/g (73 kJ/mol)] followed by clearing to the isotropic melt at 88 °C [ΔH = 1.4 J/g (2 kJ/mol)]. When low concentrations of the photoinitiator are present, these transitions are lowered by approximately 1 °C, but no other change in the phase behavior occurs. Upon cooling from the melt (10 °C/min), the isotropic to cholesteric phase transition occurs at 85−86 °C. The cholesteric phase supercools to between 50 °C and room temperature, whence crystallization to generate two crystalline forms occurs. Monomer cooled from the melt and retained at temperatures between 50 and 60 °C may remain in the cholesteric nematic phase for 1 h or more without crystallization. No smectic phase was observed for CSE-10, either on heating or on cooling.

The PCSE-10 sample used for polymer characterization was polymerized in solution as described in the Experimental Section. Polymer samples, produced by thermal polymerization of CSE-10 in solution or photopolymerization in bulk, exhibited identical textures when observed through crossed-polarizers in the optical microscope. The birefringent phase(s) of the pure polymer was observed by optical microscopy to have a fine-grained, pebbly texture and hence was very difficult to characterize by optical microscopy. Even when the polymer PCSE-10 was annealed at 150−155 °C (just below the clearing point) for several hours, no identifiable optical texture was seen since degradation of the polymer occurred.

The pure PCSE-10 polymer was examined by small angle (SAXS) and wide angle (WAXS) X-ray diffraction. The PCSE-10 polymer sample for X-ray analysis was heated to the isotropic melt at 165 °C, cooled to 90 °C and annealed (4 h), and then cooled rapidly to room temperature to "lock-in" the texture obtained by the annealing process. WAXS showed a broad, diffuse peak at $2\theta \approx 17°$ (d = 2.6 Å) and a much narrower peak at $2\theta \approx 4.5°$ (d = 10 Å). In addition to the peak at 2θ = 4.40° (d = 10.0 Å), SAXS showed an intense peak at 2θ = 2.20° (d = 20.1 Å) and a less intense peak at 2θ = 0.80° (d = 55.1 Å). These results are in agreement with the X-ray diffraction patterns reported by Shibaev et al.[30,31] for similar polymers produced from cholesteryl bearing monomers having methacrylate and acrylate reactive groups; interlayer spacings of ∼20 and 55 Å were reported.[31] Shibaev interpreted[31,32] the mesophase exhibited by the acrylate and methacrylate polymers to be a "cholesteric" phase that "possesses a pronounced layer order, and hence cannot be regarded as a twisted nematic one". It was further noted that although the layers of this structure are twisted, "each section

perpendicular to the axis of twisting represents a structure typical of the S_A phase".[32] Based on Shibaev's interpretation, we tentatively assign the PCSE-10 polymer mesophase to a phase having cholesteric optical properties, but with distinct, smectic-type layer structuring.

In an attempt to provide some assistance for understanding the nature of the medium changes occurring as polymerization progresses, aspects of the monomer/polymer phase behavior of selected monomer/polymer mixtures were analyzed. Examination by cross-polarized microscopy and DSC clearly showed that, for heating of compositions containing up to 20% PCSE-10 polymer, no obvious phase separation or texture nonuniformity occurred, either in the isotropic melt above the clearing temperature or in the cholesteric domains below the temperature. Compositions of up to 20% PCSE-10 polymer exhibited essentially all of the same transitions temperatures upon heating from 50 to 55 °C in the cholesteric phase as did the pure CSE-10 monomer. Similar results were obtained upon cooling from the melt with transition temperatures only depressed slightly for compositions containing up to ~20% polymer; i.e., a 4% PCSE-10 sample became cholesteric below 85 °C while a 17.5% polymer sample became cholesteric below 82 °C. We conclude that it is possible to determine the effect of the cholesteric nematic phase on polymerization kinetics for CSE-10 without interference from other liquid crystalline phases, as long as the polymerization conversion is maintained below about 20%.

When cooling physical monomer/polymer mixtures containing more than ~20% PCSE-10 polymer, a distinct phase change is clearly observed by DSC and optical microscopy. Upon cooling from the melt, a biphasic region composed of isotropic and liquid crystalline domains is observed which extends over a temperature range of ~30 °C. At lower temperatures, the biphasic medium appears to become a relatively uniform liquid crystalline phase. The exact assignment of the structure of the birefringent medium, either over the range where the appearance is obviously biphasic or where the more homogeneous medium occurs at lower temperature, is difficult. Based on the X-ray results for the pure PCSE-10 polymer discussed previously, we project that the homogeneous mixture at lower temperatures has smectic type layer structuring. Finally, no crystallization was observed for any CSE-10/PCSE-10 sample compositions upon cooling from the melt when samples were maintained at 55−60 °C for up to at least 15 min. Based upon this observation, no crystallization will occur during the time scale of the polymerization experiments at temperatures of 55 °C or greater.

In the next section, both free-radical and cationic polymerization at several temperatures will be followed by exotherm measurements. To substantiate phase changes which occur during the photoinitiated polymerization, data from both cross-polarized optical examination of partially polymerized samples (examined after given photolyses times), as well as the real-time continuous opacity (transmittance) measurements using a nonobtrusive HeNe light source, will be used.

B. Exotherms for Free-Radical and Cationic Photopolymerization of CSE-10. In all of the investigations involving free-radical polymerization, we note that the monomer does not absorb light at the exciting wavelengths (366 nm, 351 nm, or mercury spectrum/Pyrex filter combination) while the photoinitiator

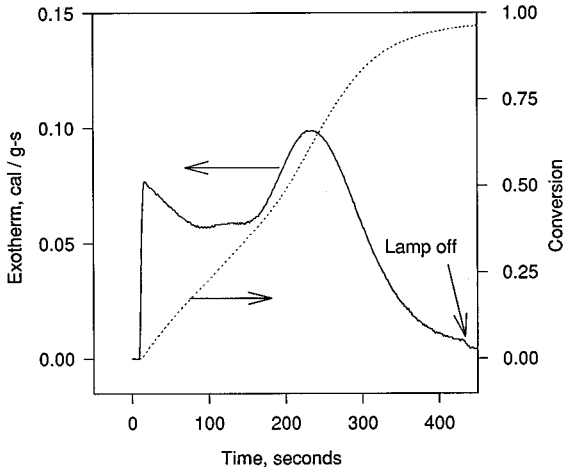

Figure 2. CSE-10 free-radical polymerization exotherm and cumulative conversion determined at 93 °C (monomer isotropic temperature, 1% DMPA photoinitiator, 366-nm filtered light, lamp intensity 0.11 mW/cm^2).

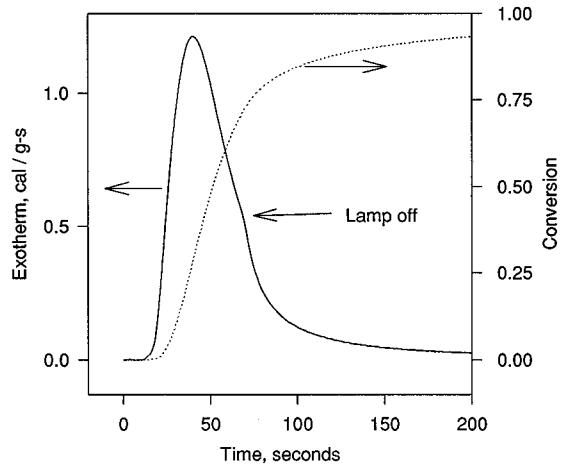

Figure 3. CSE-10 cationic polymerization exotherm and cumulative conversion determined at 93 °C [monomer isotropic temperature, 1% triaryl sulfonium salt photoinitiator, 200 ppm hydroquinone (radical inhibitor), 366-nm filtered light, lamp intensity 0.45 mW/cm^2].

(DMPA: 2,2-dimethoxy-2-phenylacetophenone) absorbs at wavelengths extending to well beyond 350 nm. Figure 2 shows the free-radical polymerization exotherm for CSE-10 at 93 °C, several degrees above the monomer clearing temperature. Initially, the exotherm resembles that expected for a well-behaved monofunctional monomer polymerized in the melt: The exotherm reaches a maximum within the instrument time response, and then decreases as the monomer is depleted. Unlike a well-behaved exotherm, however, two distinct rate accelerations are observed for the CSE-10 monomer. Similar rate accelerations occurred for polymerization of the CMA-10 acrylate monomer from the isotropic phase.[14] In contrast to the free-radical polymerization of CSE-10 (Figure 2), no sudden rate acceleration is seen in the exotherm recorded in Figure 3 for the cationic polymerization of CSE-10 (radical inhibitor added to ensure absence of free-radical polymerization) at the same temperature (93 °C). This difference in behavior can be rationalized by contrasting the two polymerization mechanisms. Although cationic and free-radical propagation mechanisms are both addition polymerization processes, there are distinct differences in the termination reactions. In free-radical polymerization, termination is bimolecular with respect to the growing

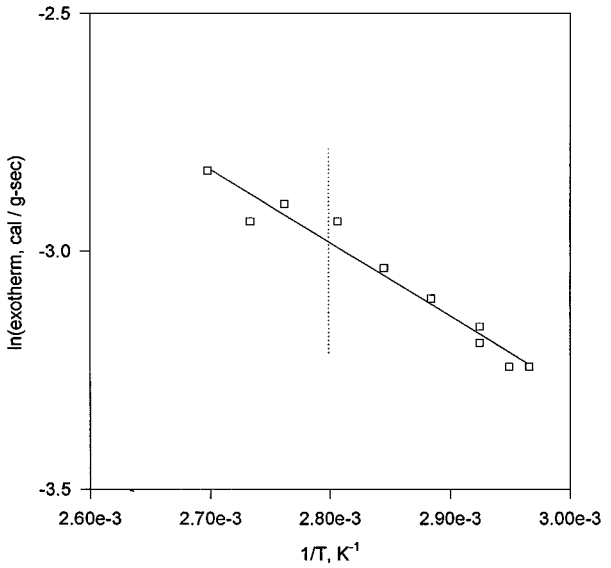

Figure 4. Arrhenius plot for initial free-radical polymerization of CSE-10, from 64 to 98 °C (1% DMPA photoinitiator, 366-nm filtered light, lamp intensity 0.24 mW/cm^2).

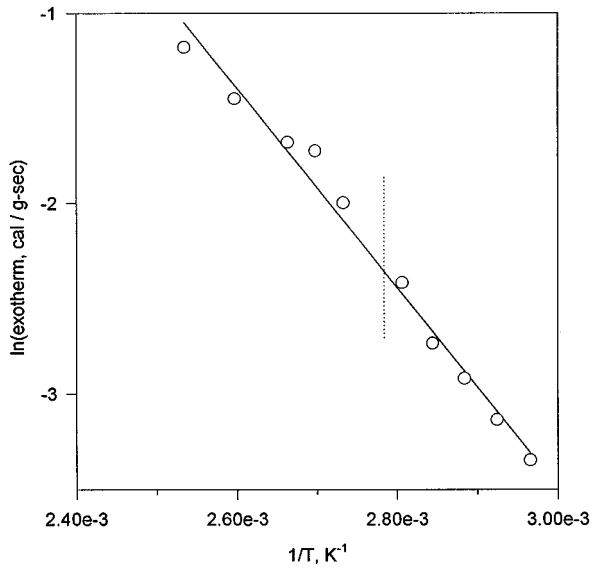

Figure 5. Arrhenius plot for cationic polymerization of CSE-10, polymerization rates measured 15 s after lamp on from 64 to 121 °C [1% triaryl sulfonium salt photoinitiator, 200 ppm hydroquinone (radical inhibitor), Pyrex filtered light, lamp intensity 4.3 mW/cm^2].

polymer chain, and hence dependent on the diffusion rate of polymer radicals. In contrast, for cationic polymerization, termination is unimolecular with respect to the growing polymer chain and thus independent of the polymer chain diffusion rate. The onset of the rate accelerations in the free-radical polymerization of CSE-10 will be shown to coincide with medium phase changes which occur during polymerization.

In order to obtain direct evidence for the effect (or absence thereof) of the monomer medium order (cholesteric nematic versus isotropic) on the free-radical polymerization rate, the log of the initial exotherm rate versus the reciprocal temperature is plotted in Figure 4. The Arrhenius plot in Figure 4 is linear (activation energy of ~3.1 kcal/mol calculated from slope) and shows no obvious discontinuity at the isotropic/cholesteric nematic transition (85−86 °C). Since polymerization at low conversions does not involve any phase changes, it is concluded that the radical termination, and hence the polymerization rate, is not affected appreciably by the cholesteric nematic phase in comparison to the isotropic phase. Apparently, the orientational ordering of the cholesteric nematic phase is not sufficient to induce a decrease in the termination rate process for the free-radical polymerization of CSE-10. In support of this conclusion, the GPC chromatograms (not shown) of polymers produced by polymerization at temperatures with the monomer in the isotropic and cholesteric nematic phases are essentially identical.

An Arrhenius plot (Figure 5) constructed from cationic polymerization rates measured after a constant photolysis time (and presumably a constant cation concentration) of 15 s (with low conversion at all temperatures) is linear, indicating that the cationic polymerization rate is not measurably affected by the medium ordering (cholesteric nematic versus isotropic). An apparent activation energy of ~10.4 kcal/mol can be calculated from the slope of the Arrhenius plot.

The analysis of the free-radical polymerization is based on the assumption that the termination rate dependence on the concentration of the growing chains is bimolecular for free-radical polymerization. To verify this assumption, we first note that, for free-radical photopolymerizations involving bimolecular termination, the polymerization rate, R_p, is related to the square root of the light intensity, $I^{1/2}$, by:

$$R_p = (k_p/k_t^{1/2}) \times [\phi f I]^{1/2} \times [M] \qquad (1)$$

where k_p and k_t are the rate constants for propagation and termination, ϕ is the quantum efficiency for production of radical initiators, f is the fraction of light absorbed at the excitation wavelength, and [M] is the monomer concentration. Linear log−log plots of the initial (low conversion free-radical) polymerization rate versus light intensity at 69 °C (cholesteric nematic phase) and 93 °C (isotropic phase) have slopes of 0.54 and 0.55, indicating that (within experimental error) termination is bimolecular for CSE-10 in the early stages of polymerization in both the cholesteric nematic and isotropic phases. The cholesteric nematic phase organization apparently does not alter the basic bimolecular termination mechanism.

Pulsed laser-initiated polymerization has been shown to be an effective tool for probing free-radical polymerization at low conversions.[33−47] We determined the effect of laser pulsing frequency on the molecular weight distribution of CSE-10 polymer formed at 69 and 93 °C (cholesteric nematic and isotropic phases) by selective irradiation of samples with 50 total laser pulses (351 nm, 3.6 mJ/cm^2 pulse) at a variety of repetition rates. In all cases the conversion to polymer was low: less than 10%. Figures 6 and 7 present the GPC data for the polymer samples produced from polymerization CSE-10 at 69 °C (cholesteric nematic phase) and 93 °C (isotropic phase) at several laser repetition rates. At both temperatures, the GPC peak retention time shifts to longer times with increasing laser repetition rate, indicating the presence of substantial premature termination in both the isotropic and cholesteric nematic phases as the time between laser pulses decreases. (See refs 33−35 for details of this phenomenon in isotropic systems.) The molecular weight distribution for polymer generated at 0.1 Hz at either temperature resembles the broad distribution typical of purely isotropic systems. We note that retention times for the polymers produced by polymerization at 93 °C are slightly shorter than those at 69 °C, consistent with the observation that

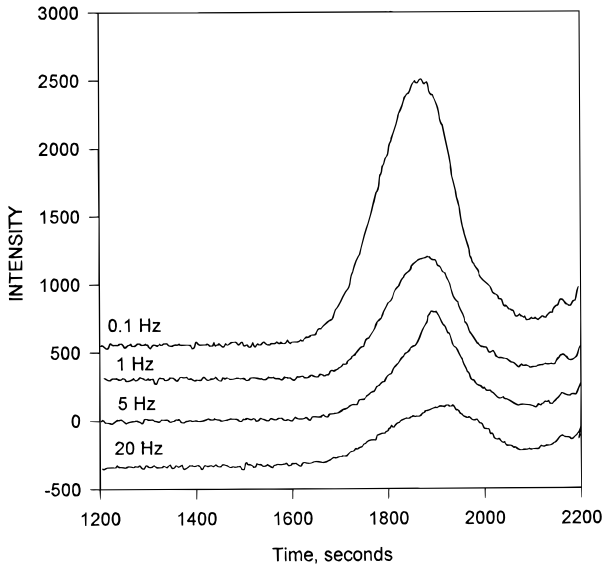

Figure 6. GPC of CSE-10 polymer, low conversion, made at 69 °C by 50 laser pulses at various laser repetition rates (monomer cholesteric nematic phase on cooling; $\lambda = 351$ nm, laser power per pulse 3.6 mJ/cm^2).

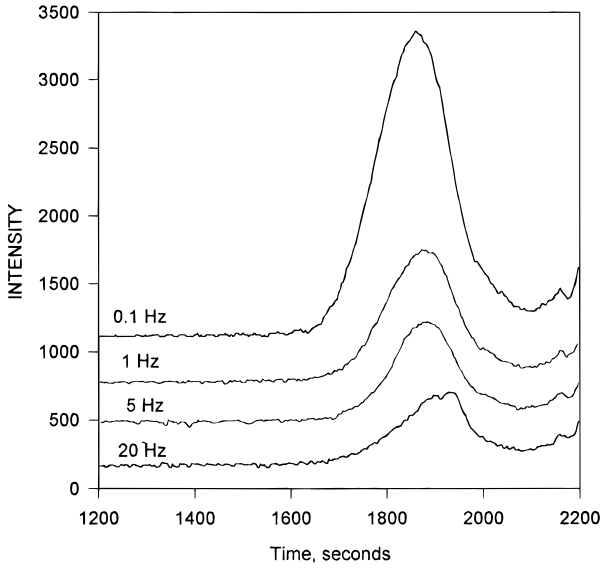

Figure 7. GPC of CSE-10 polymer, low conversion, made at 93 °C by 50 pulses at various laser repetition rates (monomer isotropic phase; $\lambda = 351$ mn, laser power per pulse 3.6 mJ/cm^2).

the polymerization rate and quantum efficiency are greater at higher temperatures. At higher repetition rates for polymerization at both 69 and 93 °C, additional low molecular weight peaks appear at longer retention times (due to termination between polymer radical chains and primary radicals) and increase in magnitude (relative to the higher molecular weight peaks in the same sample) as the repetition rates increases. As in the case of samples produced with the continuous light source mentioned earlier, the molecular weight distributions for a given repetition rate are essentially identical upon polymerization in the isotropic and cholesteric nematic phases. The results of the pulsed laser-initiated polymerization thus indicate that there is no significant difference between polymerization in the isotropic and cholesteric nematic phases of the CSE-10 monomer with respect to termination involving small molecule radicals and growing polymer chains. The results for CSE-10 are substantially different from the free-radical polymerization of CMA-10 in the smectic A phase, where little premature termination occurs, and the molecular weight produced is independent of the laser repetition rate.[14]

Returning to the polymerization exotherm for CSE-10 at 93 °C (Figure 2), we note the initial very modest rate acceleration which occurs at about 20−25% conversion. For an independent monomer/polymer mixture we found that, at approximately 20−25 percent conversion, a phase separation/phase change first occurred producing a nonhomogeneous biphasic medium. Apparently, this medium produces a minor rate acceleration, probably resulting from a small decrease in termination rate. The major polymerization rate acceleration at 93 °C begins at about 35−40% conversion, reaches a midpoint at about 50% conversion, and finally attains a peak maximum at approximately 60−65% conversion. Interestingly, we observed that independently prepared mixtures exhibited a relatively uniform liquid crystalline texture for mixtures of about 35−40% polymer at temperatures between 90 and 95 °C, but a clearly biphasic mixture for lower polymer compositions between 20% and 35%. We observed (via cross-polarized optical microscopic examination) a change in appearance of the CSE-10 polymerization medium from an isotropic melt to a uniform pebbly texture (probably smectic) after a given period of irradiation, long enough to ensure high conversion (>35−40%). An identical change in medium texture was also noted (via cross-polarized microscopic examination) for the cationic polymerization: The lack of a sudden rate acceleration in the cationic polymerization compared to the free-radical polymerization must originate from differences in the termination mechanisms for the two cases as discussed earlier. Interestingly, Jahromi et al. recently reported that the cationic ring opening polymerization of a liquid crystalline diepoxide experienced a rate increase during polymerization corresponding to a transition from an isotropic to a nematic medium.[48] They attributed the increase to a lower activation energy for propagation in the liquid crystalline phase. The propagation mechanisms for styryloxy (addition of cationic chain to double bond) and epoxy (ring opening) cationic polymerization are quite different and could possibly account for the rate acceleration found in one case (epoxy) and not the other (styryloxy). Presumably, in the case of cationic polymerization, termination, which does not involve interaction of two growing polymer chains, is apparently not affected by the medium change in either case.

Turning next to free-radical polymerization at 69 °C (Figure 8), a major rate acceleration begins at about 15−20% conversion, attains a midpoint rate at about 30−32% conversion, and reaches a maximum rate at about 45−50% conversion. (As at 93 °C, there appears to be a very minor rate acceleration that occurs prior to the major rate acceleration.) The shape of the cationic polymerization exotherm at 69 °C (not shown) was similar to that observed at 93 °C (Figure 3), with no sudden rate acceleration observed. Large scale texture changes occur when CSE-10 monomer in the oily cholesteric phase at 69 °C is photopolymerized by either a free-radical or cationic process. The medium, observed by cross-polarized optical microscopy, changes from a typical oily cholesteric medium to a multicolored, pebbly texture similar to that ultimately observed at higher conversions for polymerization at temperatures (90−95 °C) where the initial phase is isotropic. The medium

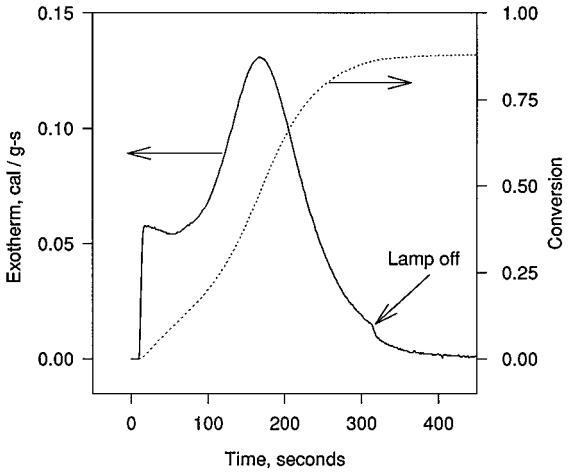

Figure 8. CSE-10 free-radical polymerization exotherm and cumulative conversion measured at 69 °C (monomer cholesteric nematic phase on cooling; 1% DMPA photoinitiator, 366-nm filtered light, lamp intensity 0.11 mW/cm^2).

ultimately attains a relatively homogeneous liquid crystalline texture (probably smectic) in both cases.

In order to correlate the rate accelerations for the free-radical polymerization at 69 and 93 °C to changes in polymerization media, simultaneous measurements of the polymerization exotherm and medium clarity were recorded using the apparatus shown in Figure 1 (previously described in the Experimental Section). Monomer samples were first analyzed to confirm that the thermal transitions due to phase changes measured by DSC corresponded to intensity changes in the transmitted HeNe laser light reflected through the samples. For both heating and cooling, a substantially greater transmitted light intensity occurred in the isotropic melt, which was highly transparent. Based on this, we anticipate that it should be relatively straightforward to observe an isotropic to liquid crystalline phase change during polymerization via changes in medium clarity. A significantly smaller increase in the transmitted light intensity occurred when the crystalline monomer melted to the cholesteric liquid crystalline phase. Hence, by analogy we may project that some difficulty may be encountered in detecting changes during polymerization from the initial pure cholesterol nematic phase of the monomer to another liquid crystalline phase(s) if the optical clarity differences are not large. Plots of the polymerization exotherm, conversion versus time, and transmitted light intensity versus time for free-radical polymerization of CSE-10 at 69 and 93 °C are presented in Figures 9 and 10. Considering first the results at 69 °C, we note a change (Figure 9) in the transmitted light intensity of the sample polymerized from the cholesteric nematic phase (69 °C) beginning at about 15−20% conversion. The transmitted light intensity change corresponds to the large rate acceleration and change in medium texture noted previously via optical microscopy. The small decrease in transmitted light intensity accompanying the medium change upon proceeding from the cholesteric nematic is rather difficult to detect and reflects the relative efficiency of both phases in scattering the HeNe probe light. After the initial decrease, the transmitted light intensity decreases slowly as the polymerization progresses.

Results for free-radical polymerization from the isotropic monomer phase at 93 °C (Figure 10) show a clear distinct decrease in the transmitted light intensity corresponding to the percent conversion for onset of the

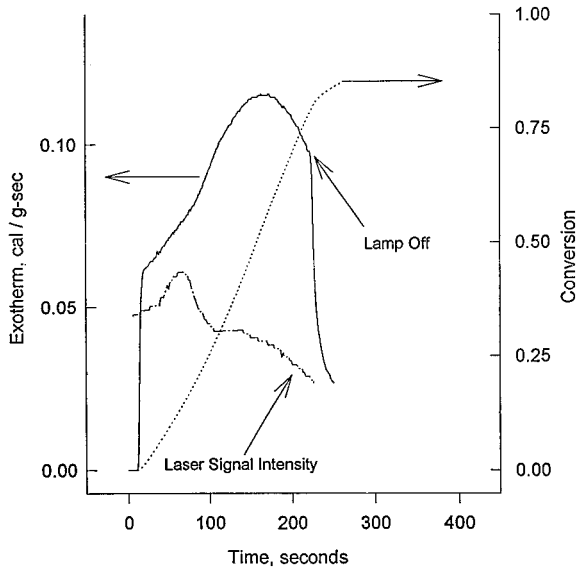

Figure 9. CSE-10 free-radical polymerization exotherm [cal/(g•s)], cumulative conversion, and simultaneous transmitted light intensity signal obtained during polymerization at 69 °C (monomer cholesteric nematic phase on cooling; 1% DMPA photoinitiator, Pyrex filtered light, lamp intensity 1.2 mW/cm^2).

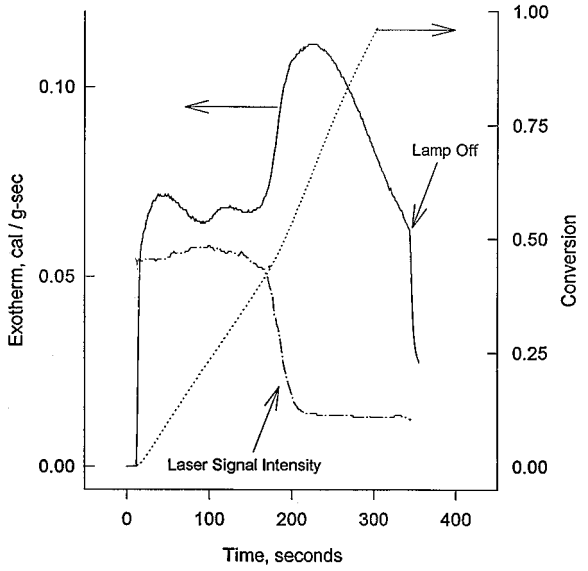

Figure 10. CSE-10 free-radical polymerization exotherm [cal/(g•s)], cumulative conversion, and simultaneous transmitted light intensity signal obtained during polymerization at 93 °C (monomer isotropic phase; 1% DMPA photoinitiator, Pyrex filtered light, lamp intensity 0.6 mW/cm^2).

larger of the two rate accelerations in the polymerization exotherm. The rapid decrease in the transmitted HeNe light intensity begins at about 35% conversion and continues until a conversion of approximately 50−55% is attained: Additional conversion leads to no additional decrease in transmitted light intensity. These results agree with results for various monomer/polymer physical mixtures which show that at about 45−50% polymer (at 93 °C) a uniform grainy, pebbly texture is achieved. Apparently, the rate increase occurs as the medium changes from one with isotropic order to one which has substantial liquid crystalline order. The smaller rate acceleration previously noted to occur at the lower conversion (∼20%) is not accompanied by any detectable change in the transmitted light intensity signal (within the limits of the resolution of our system). Interestingly,

if the lamp is terminated either just before or just after the smaller rate acceleration at ~20% conversion, no change is observed in the transmitted light intensity with time, since there is little dark polymerization or any reorganization of the sample with time. Cooling of these partially converted (approximately 20%) samples from 93 °C results in a large decrease in the transmitted light intensity at about 85 °C, accompanied by a thermal transition (DSC) similar to that observed for the isotropic to cholesteric nematic transition of the pure monomer. This suggests that, both prior to and just after the minor rate acceleration at ~20% conversion at 93 °C, the bulk of the medium is mainly isotropic in nature. This is in accordance with the previous postulation that the medium giving rise to the small rate acceleration at 20% conversion is primarily isotropic with a small amount of a low order mesogenic phase present (the latter is suggested by optical microscopic examination). At 93 °C, if irradiation is terminated just prior to the beginning of the second rate acceleration (32% conversion), the transmitted light signal intensity falls, and continues to decrease over a much larger time scale (several minutes) than the exotherm decay (<20 s). This indicates that a small amount of dark polymerization leading to a medium phase change and a large amount of medium reorganization are occurring with time. Interestingly, when this sample is cooled, no change in transmission is seen at 85 °C due to an isotropic−liquid crystalline phase transition, nor are any other transitions in the DSC cooling curve recorded. Finally, at 93 °C when the lamp is terminated after the major rate acceleration begins and the medium becomes highly scattering, no change is observed in the intensity of light transmitted through the sample with time. Also, no change occurs in the transmitted light intensity signal or DSC exotherm transition due to a monomer phase transition at ~85 °C as the sample is cooled.

In order to confirm that cationic polymerization causes the same changes in polymerization media as for the free-radical polymerization, CSE-10 cationic polymerization exotherms were observed concurrent with transmitted light intensity measurements, just as for the free-radical polymerization. Plots of the polymerization exotherm, percent conversion, and the transmitted light intensity versus time for cationic polymerization of CSE-10 at 69 and 93 °C are presented in Figures 11 and 12, respectively. The change (decrease) in transmitted light intensity observed at 69 °C for the cationic polymerization begins at almost the same conversion as for the free-radical polymerization (~20%). In contrast to the free-radical polymerization, when the lamp is terminated for the cationic polymerization at slightly less than 20% conversion, there is a subsequent decrease (not shown) in the transmitted light intensity. The transmitted light intensity does not decrease as rapidly as when the lamp exposure is continued, but it does decrease on about the same time scale as the exotherm decay (measured for samples without the HeNe laser). Clearly, substantial dark polymerization occurs for the cationic polymerization, accompanied by the subsequent medium change when 20% conversion is attained. (The continued formation of polymer after terminating the light source was verified by quenching experiments, which are not discussed in this paper.)

When cationic polymerization is initiated in the isotropic phase at 93 °C, a distinct decrease in the transmitted light intensity is observed at ~35% conversion (Figure 12), just as for the free-radical polymerization at a similar conversion. If the lamp is terminated just prior to the decrease in the transmitted light intensity, a decrease in the signal continues as the dark polymerization proceeds and phase change occurs.

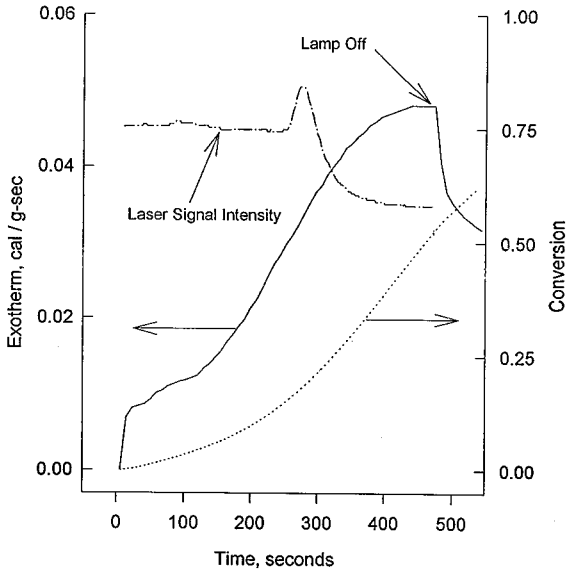

Figure 11. CSE-10 cationic polymerization exotherm [cal/(g·s)], cumulative conversion, and simultaneous transmitted light intensity signal obtained during polymerization at 69 °C (monomer cholesteric nematic phase on cooling; 1% triaryl sulfonium salt cationic photoinitiator and 200 ppm hydroquinone, Pyrex filtered light, lamp intensity 1.2 mW/cm^2).

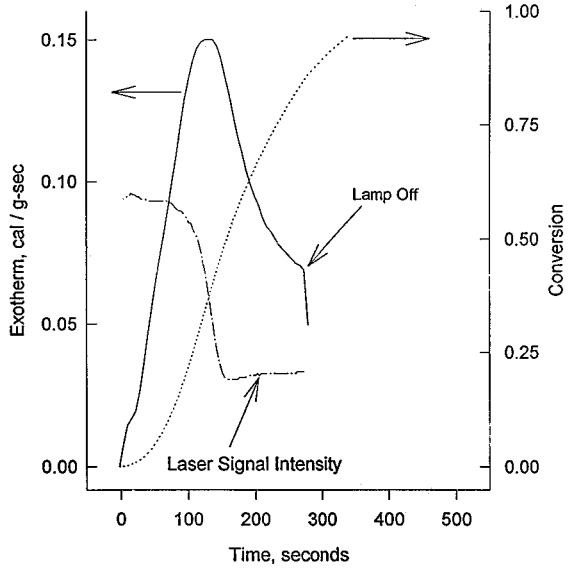

Figure 12. CSE-10 cationic polymerization exotherm [cal/(g·s)], cumulative conversion, and simultaneous transmitted light intensity signal obtained during polymerization at 93 °C (monomer isotropic phase; 1% triaryl sulfonium salt cationic photoinitiator and 200 ppm hydroquinone, Pyrex filtered light, lamp intensity 2.5 mW/cm^2).

In summary, the light scattering analysis suggests that, although rate acceleration only occurs during free-radical polymerization, similar phase changes occur during both cationic and free-radical polymerization. This is in accordance with the presumption of a reduction in the bimolecular termination rate for free-radical polymerization commensurate with a medium phase change.

C. Kinetic Measurements. In a previous investigation of CMA-10, we found that when the polymerization medium changed from an isotropic to a smectic

Table 1. Ratio of Propagation Rate Constant to Termination Rate Constant for Free-Radical Polymerization of CSE-10 at 69 °C[a]

% conversion range	k_t/k_p	% conversion range	k_t/k_p
0−15	>400[b]	40−50	55
20	250	50−60	35
25	155	75−85	15
35	70		

[a] Polymerization medium is initially in cholesteric nematic phase. [b] Due to difficulty in measuring very rapid decay rates, the value for k_t/k_p is a lower limit value at this conversion.

Table 2. Ratio of Propagation Rate Constant to Termination Rate Constant for Free-Radical Polymerization of CSE-10 at 93 °C[a]

% conversion range	k_t/k_p	% conversion range	k_t/k_p
0−30	>400[b]	65−75	60
35−45	220	75−80	25
50−65	85		

[a] Polymerization medium is initially isotropic. [b] Due to difficulty in measuring very rapid decay rates, the value for k_t/k_p is a lower limit value at this low conversion.

dominated medium, the ratio k_t/k_p decreased dramatically.[14] The decrease in the k_t/k_p ratio was found to result from a marked decrease in k_t. The ratio k_t/k_p can be readily determined for CSE-10 in a manner similar to that employed for CMA-10 by simply terminating the polymerization light source and recording the decay of the non-steady-state exotherm with time (t), which proceeds according to the following equation, originally presented by Tryson and Schultz:[23,24]

$$\frac{[M]}{(-d[M]/dt)} = \frac{k_t}{k_p}t + \frac{[M]_0}{(-d[M]/dt)_0} \qquad (2)$$

where [M] is the monomer concentration, $-d[M]/dt$ is the polymerization rate determined from the measured DSC exotherm, k_t is the termination rate constant, k_p is the propagation rate constant, and $[M]_0$ and $(-d[M]/dt)_0$ are the monomer concentration and the polymerization rate, respectively, at the instant that the polymerization light source is removed. Using eq 2, the ratio k_t/k_p can be obtained from the slope of linear plot of $[M]/(-d[M]/dt)$ versus t. At the instant that the light is terminated, $t = 0$.

Tables 1 and 2 list numerous k_t/k_p ratios calculated at 69 and 93 °C as a function of conversion to polymer. At both temperatures, the ratio k_t/k_p is quite large at low conversions (prior to the rate acceleration). In each case (69 and 93 °C), the decrease in the k_t/k_p ratio is concurrent with the rate acceleration and decrease in transmitted HeNe light intensity values noted in Figures 9 and 10. If, as is the case for CMA-10, we assume that k_p is chemically, rather than diffusion, controlled, our results would then indicate that the rapid drop in the k_t/k_p ratio is due to the decrease in k_t as polymer radical chain diffusion becomes slower after the medium phase change occurs.

Conclusions

The photoinitiated polymerization of a liquid crystalline styryloxy monomer with a cholesteryl mesogen attached to the styryloxy monomer unit via a methylene chain (10 CH_2 units) has been investigated in both isotropic and cholesteric nematic phases. Using a nonobtrusive HeNe light scattering probe and observation via cross-polarized optical microscopy, it is determined that a homogeneous phase (either isotropic or cholesteric nematic, depending upon the temperature of the sample) is maintained, with no phase changes or phase separation, to ~20% conversion (or greater when beginning from the isotropic phase) over a wide temperature range. An accompanying Arrhenius analysis of rate data at low conversions demonstrated that the cholesteric nematic phase does not cause any unexpected changes in the free-radical polymerization rate. The rate data were verified by analysis of polymer molecular weight distributions of samples generated from low conversions in the cholesteric nematic and isotropic phases using both continuous mercury lamp and pulsed laser sources to initiate polymerization.[49]

A combination of the HeNe laser light scattering probe to measure medium transmittance and continuous exotherm analysis indicated that a rate acceleration for the free-radical polymerization accompanied a phase change from either the cholesteric nematic or isotropic phase to a medium with enhanced (probably similar to that of the pure polymer) ordering. The rate acceleration is postulated to arise from a decrease in the termination rate constant which accompanies the media phase changes.

Acknowledgment. We acknowledge the National Science Foundation (Grant DMR-8917485 Polymers Program and the EPSCoR Program) and the University of Southern Mississippi for support of this work.

References and Notes

(1) Percec, V.; Johnson, H.; Tomazos, D. In *Polymerizations in Organized Media*; Paleos, C. M., Ed.; Gordon and Breach Science Publishers: Philadelphia, 1992; p 1.
(2) Paleos, C. M. *Chem. Soc. Rev.* **1985**, *14*, 45.
(3) Barrall, E. M.; Johnson, J. F. *J. Macromol. Sci., Rev. Macromol. Chem.* **1979**, *17*, 137.
(4) Blumstein, A. *Midl. Macromol. Monogr.* **1977**, *3*, 133.
(5) Broer, D. J.; Mol, G. N.; Challa, G. *Makromol. Chem.* **1989**, *190*, 19.
(6) Broer, D. J.; Boven, J.; Mol, G. N.; Challa, G. *Makromol. Chem.* **1989**, *190*, 2255.
(7) Broer, D. J.; Mol, G. N. *Makromol. Chem.* **1991**, *192*, 59.
(8) Broer, D. J.; Finkelmann, H.; Kondo, K. *Makromol. Chem.* **1988**, *189*, 185.
(9) Broer, D. J.; Hikmet, R. A. M.; Challa, G. *Makromol. Chem.* **1989**, *190*, 3201.
(10) Hoyle, C. E.; Kang, D.; Chawla, C. P.; Griffin, A. C. *Polym. Eng. Sci.* **1992**, *32*, 1490.
(11) Kang, D. Ph.D. Dissertation, University of Southern Mississippi, 1992.
(12) Hoyle, C. E.; Chawla, C. P.; Kang, D.; Griffin, A. C. *Macromolecules* **1993**, *26*, 758.
(13) Hoyle, C. E.; Kang, D. *Macromolecules* **1993**, *26*, 844.
(14) Hoyle, C. E.; Watanabe, T. *Macromolecules* **1994**, *27*, 3790.
(15) Paleos, C. M.; Labes, M. M. *Mol. Cryst. Liq. Cryst.* **1970**, *11*, 385.
(16) Perplies, E.; Ringsdorf, H.; Wendorf, J. H. *Makromol. Chem.* **1974**, *175*, 533.
(17) Hus, E. C.; Blumstein, A. *J. Polym. Sci., Polym. Lett. Ed.* **1977**, *15*, 129.
(18) Hoyle, C. E.; Chawla, C. P.; Griffin, A. C. *Mol. Cryst. Liq. Cryst. Incorporating Nonlinear Opt.* **1988**, *157*, 639.
(19) Jonsson, H. Ph.D. Dissertation, Royal Institute of Technology, 1991.
(20) Shannon, P. J. US Patent 4,614,782, 1986.
(21) Shannon, P. J. *Macromolecules* **1983**, *16*, 1677.
(22) Corson, B. B.; Heintzelman, W. J.; Schwartzman, L. H.; Tiefenthal, H. E.; Lokken, R. J.; Nickels, J. E.; Atwood, G. R.; Pavlik, F. J. *J. Org. Chem.* **1958**, *23*, 544.
(23) Tryson, G. R.; Schultz, A. R. *J. Polym. Sci., Polym. Phys. Ed.* **1979**, *17*, 2059.
(24) Schultz, A. R.; Tryson, G. R. *J. Polym. Sci., Polym. Phys. Ed.* **1984**, *22*, 1753.
(25) Crivello, J. V.; Lam, J. H. W. *J. Polym. Sci., Polym. Lett. Ed.* **1979**, *17*, 759.
(26) Matjaszewski, K. In *Comprehensive Polymer Science: Volume 3, Chain Polymerization I*; Eastmond, G. C., Ledwith, A.,

Russo, S., Sigwalt, P., Eds.; Pergamon Press: Oxford and New York, 1989; p 639.
(27) Cowie, J. M. G. Page 11 In ref 26.
(28) Demus, D.; Richer, L. *Textures of Liquid Crystals*; Verlag Chemie: New York, 1978.
(29) Gray, G. W.; Goodby, J. W. G. In *Smectic Liquid Crystals—Textures and Structures*; Leonard Hill: Glasgow and London, 1984; p 21.
(30) Platé, N. A.; Shibaev, V. P. In *Comb-Shaped Polymers and Liquid Crystals*; Plenum Press: New York, 1987; p 356.
(31) Freidzon, Ya. S.; Shibaev, V. P.; Kharitonov, A. V.; Platé, N. A. In *Advances in Liquid Crystal Research and Applications*; Bata, L., Ed.; Pergamon Press: Oxford, 1980; p 899.
(32) Shibaev, V. P.; Freidzon, Ya. S.; Lomonosov, M. V. In *Side Chain Liquid Crystal Polymers*; McArdle, C. B., Ed.; Blackie and Sons Ltd.: Glasgow and London, 1989; p 260.
(33) Davis, T. P. *J. Photochem. Photobiol., A* **1994**, *77*, 1.
(34) Olaj, O. F.; Schnoll-Bitai, I. *Angew. Makromol. Chem.* **1987**, *155*, 177.
(35) McLaughlin, K. W.; Latham, D. D.; Hoyle, C. E.; Trapp, M. A. *J. Phys. Chem.* **1989**, *93*, 3643.
(36) Olaj, O. F.; Bitai, I.; Gleixner, G. *Makromol. Chem.* **1985**, *186*, 2569.
(37) Olaj, O. F.; Bitai, I.; Hinkelmann, F. *Makromol. Chem.* **1987**, *188*, 1689.
(38) Olaj, O. F.; Bitai, I. S. *Makromol. Chem., Rapid Commun.* **1988**, *9*, 275.
(39) Bitai, I. S.; Zifferer, G.; Olaj, O. F. *Makromol. Chem., Rapid Commun.* **1988**, *9*, 659.
(40) Davis, T. P.; O'Driscoll, K. F.; Piton, M. C.; Winnik, M. A. *Macromolecules* **1989**, *22*, 2785.
(41) Davis, T. P.; O'Driscoll, K. F.; Piton, M. C.; Winnik, M. A. *J. Polym. Sci., Polym. Lett. Ed* **1989**, *27*, 181.
(42) Davis, T. P.; O'Driscoll, K. F.; Piton, M. C.; Winnik, M. A. *Macromolecules* **1990**, *23*, 2113.
(43) Hoyle, C. E.; Trapp, M. A.; Chang, C. H.; Latham, D. D.; McLaughlin, K. L. *Macromolecules* **1898**, *22*, 35.
(44) Hoyle, C. E.; Trapp, M. A.; Chang, C. H. *J. Polym. Sci., Polym. Chem. Ed.* **1989**, *27*, 1989.
(45) Hoyle, C. E.; Chang, C. H.; Trapp, M. A. *Macromolecules* **1989**, *22*, 3607.
(46) Olaj, O. F.; Schnoll-Bitai, I. *Eur. Polym. J.* **1989**, *25*, 635.
(47) Davis, T. P.; O'Driscoll, K. F.; Piton, M. C.; Winnik, M. A. *Polym. Int.* **1991**, *24*, 65.
(48) Jahromi, S.; Lub, J.; Mol., G. N. *Polymer* **1994**, *35*, 622.
(49) We note, as aptly pointed out by a reviewer, that a general statement about polymerization rates in nematic versus isotropic phases cannot be made based simply on one example. It may be that a shorter spacer between the reactive monomer and the mesogenic unit would result in a more ordered monomer with specific rate consequences in addition to a simple viscosity effect on rate processes. In addition, the results in this report are for a cholesteric nematic phase, and differences might arise in some cases for polymerization in classical nematic phases.

MA950826Z